Monitoring of offshore wind turbine monopiles for life extension

Jinsheng Wang [a], Paul Fromme [a], Philippe Duffour [b]
[a] Department of Mechanical Engineering, University College London, London, WC1E 7JE, UK;
[b] Department of Civil, Environmental and Geomatic Engineering, University College London, London, WC1E 7JE, UK

ABSTRACT

The rapid expansion of offshore wind electricity generation capacity over the past decades means that many existing wind farms will soon come to the end of their design life, typically using monopiles as the support structure in medium water depths. The need for renewable energy generation and lower embodied carbon will in many cases encourage offshore wind turbine life extension. The viability for lifetime extension was investigated using reliability analysis, leveraging a novel active learning framework with an ensemble of surrogate models and offering valuable insights for risk-based decision-making and sustainable management of offshore wind assets. For a reference monopile-supported OWT, this provided accurate failure probability estimates with significantly reduced computational costs. Results indicate a progressive decline in OWT reliability over time due to accumulated fatigue damage under cyclic environmental loading. The feasibility of employing guided ultrasonic waves to monitor the inaccessible, submerged part of the monopiles to detect the development of critical defects was explored to assess the sensitivity for typical fatigue and corrosion defects at circumferential welds. The guided wave sensor data could be combined with wind and wave load predictions to facilitate fatigue reliability analysis based on structural health monitoring.

Keywords: Guided ultrasonic waves, offshore wind turbine, fatigue reliability analysis, renewable energy, structural health monitoring

1. INTRODUCTION

Offshore wind turbines (OWTs) are a crucial component for the shift towards renewable energy, playing a pivotal role in reducing carbon emissions and meeting long-term sustainability targets [1]. Monopile-supported OWTs are the most common offshore installation due to their cost-effectiveness and adaptability up to medium water depths. However, their structural integrity needs to be ascertained, as cyclic wind, wave, and operational loads can lead to progressive fatigue damage [2]. Ensuring the long-term reliability of these structures is essential for extending service life and reducing lifecycle costs [3]. Fatigue failure in OWT monopiles primarily stems from repeated stress cycles caused by dynamic loading, with critical regions often located near circumferential welds below the mudline. Accurately assessing fatigue life requires a comprehensive understanding of environmental conditions, material behavior, and loading uncertainties [4].

Conventional fatigue assessment methods mainly rely on time-domain simulations coupled with cumulative damage models such as the Palmgren-Miner rule. While effective, these approaches are computationally expensive, particularly for long-term reliability assessments under varying load conditions [5]. To address these challenges, researchers have explored surrogate-based approaches for efficient fatigue reliability analysis [6]. The commonly used surrogate models include the response surface method, artificial neural network, polynomial chaos expansion, and Kriging model [7-9]. However, current surrogate-based methods often rely on one-shot sampling techniques, where training samples are generated beforehand using space-filling designs. This approach fails to dynamically focus on the most critical areas of the design space, particularly regions near the failure boundaries or those with high uncertainty [10]. Consequently, computational resources may be inefficiently allocated, and the accuracy of fatigue reliability predictions can be compromised. Moreover, single surrogate models may struggle to capture the complexities and nonlinearity inherent in fatigue damage predictions for OWTs, especially under varying environmental conditions [11].

To overcome these limitations, this study proposes the use of ensemble surrogate models, which combine multiple individual models to leverage their complementary strengths. By integrating different types of surrogates, such as Kriging [7], Bayesian Support Vector Regression (BSVR) [12], and Polynomial Chaos Kriging (PCK) [13], the ensemble approach enhances prediction accuracy and robustness, better capturing the complex relationships between environmental factors and structural responses. Additionally, active learning strategies are introduced to iteratively select the most informative training samples, focusing on the regions with high uncertainty or near the critical failure points. This dynamic sampling process ensures that the model is refined efficiently, reducing the need for excessive function evaluations and improving computational efficiency. Through the combination of ensemble models and active learning, the proposed approach offers a more accurate, adaptable, and resource-efficient solution for fatigue reliability analysis of OWTs.

Structural Health Monitoring (SHM) techniques, particularly guided ultrasonic waves, offer a promising solution for real-time fatigue damage assessment. These techniques could enable the detection of defects in submerged monopile sections, where direct inspection is challenging. By integrating SHM data with probabilistic fatigue models, the predictive capabilities could be enhanced and proactive maintenance strategies developed, ultimately supporting the life extension of offshore wind assets. This study proposes a novel framework combining guided wave-based SHM with an adaptive ensemble of surrogate models for efficient fatigue reliability analysis of monopile-supported OWTs. The methodology is designed to improve fatigue life predictions, reduce computational costs, and support risk-informed decision-making for sustainable offshore wind farm management.

2. NUMERICAL MODEL OF A REFERENCE OWT

To evaluate the fatigue reliability of OWTs, a robust numerical model is required to capture the complex interactions between structural dynamics and environmental forces. This study utilizes the well-known NREL 5 MW monopile-supported reference OWT [14] for the case study, as shown in Fig. 1a.

The finite element (FE) model of the referenced OWT employs Euler-Bernoulli beam elements to represent the tower/monopile [15]. Each node has six degrees of freedom (DOFs), encompassing three translational and three rotational motions. Rayleigh damping is introduced to account for both structural and soil damping, while the nacelle is modeled as a lumped mass at the tower top, simplifying computations by assuming no rotational inertia. The soil-structure interaction is captured using lateral soil springs formulated based on *p-y* curves. Aerodynamic forces are determined via unsteady blade element momentum theory, while hydrodynamic loads are computed using Morison's equation. The governing equation of motion for the coupled system is formulated as described in more detail in [15]:

$$\mathbf{M}(t)\ddot{\mathbf{u}}(t) + \left(\mathbf{C}_{\text{Struc}}(t) + \mathbf{C}_{\text{Soil}}(t)\right)\dot{\mathbf{u}}(t) + \mathbf{K}(t)\mathbf{u}(t) = \mathbf{F}_{\text{Wind}}(t) + \mathbf{F}_{\text{Wave}}(t) \tag{1}$$

where $\mathbf{u}(t)$ represents the displacement vector, $\mathbf{M}(t)$, $\mathbf{C}_{\text{Struc}}(t)$, $\mathbf{C}_{\text{Soil}}(t)$ and $\mathbf{K}(t)$ are the time-dependent mass, damping, and stiffness matrices. External forces $\mathbf{F}_{\text{Wind}}(t)$ and $\mathbf{F}_{\text{Wave}}(t)$ correspond to wind and wave loads.

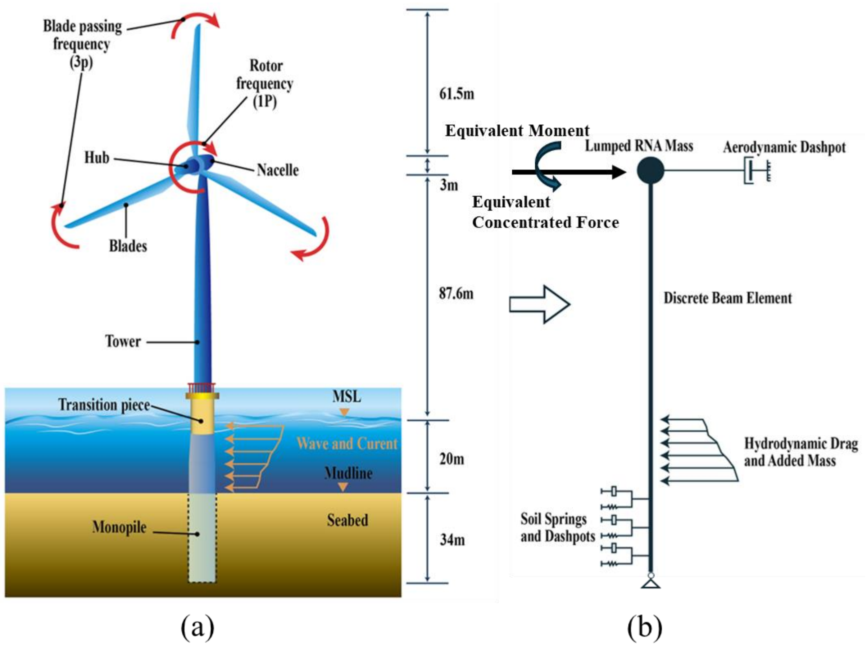

Figure 1. Schematics of: (a) 5 MW monopile-supported reference OWT; (b) corresponding numerical model.

To enhance computational efficiency, an aerodynamically decoupled approach is employed, where the aerodynamic forces from the rotor are linearized at the tower top. This introduces an additional aerodynamic damping matrix, which captures the interactions between fore-aft and side-side motions of the turbine. By employing this approach, the computational cost is significantly reduced, while maintaining high accuracy in fatigue life predictions. The numerical model is shown in Fig. 1b, and the application of the HHT-α method (extension of the Newmark-β method) ensures numerical efficiency, stability and accuracy. For further details on the numerical model, please refer to [15].

3. RELIABILITY ANALYSIS WITH ADAPTIVE ENSEMBLE OF SURROGATES

This section introduces a new method for structural reliability analysis using an adaptive ensemble of surrogate models (AEOS), with the overall workflow depicted in Fig. 2. In this approach, multiple surrogate models are combined into a single ensemble model, where each model is assigned a weight that reflects its contribution to the overall prediction. The ensemble model $\hat{g}_E(\boldsymbol{x})$ is expressed as follows:

$$\hat{g}_E(\boldsymbol{x}) = \sum_{i=1}^{m} w_i \hat{g}_i(\boldsymbol{x}), \quad \text{where} \quad \sum_{i=1}^{m} w_i = 1 \tag{2}$$

where $\hat{g}_i(\boldsymbol{x})$ represents the i-th surrogate model, w_i is its corresponding weight factor, and m denotes the total number of surrogate models in the ensemble. In this study, three surrogate models (Kriging, BSVR, and PCK) are used, each chosen for their unique advantages.

Unlike traditional AEOS methods where weights calculation is primarily focused on global error metrics, both global error E_i^G (in terms of leave-one-out-error) and local error E_i^L (in terms of the sum of prediction variance in critical regions) are considered to determine the appropriate weights for each model. The weight factor w_i for each surrogate in the AEOS can be calculated using the following equation:

$$w_i = \frac{w_i^*}{\sum_{j=1}^{m} w_j^*}, \quad \text{where} \quad w_i^* = \frac{\exp(-10E_i^L)}{E_i^G}, \; i = 1,2,\ldots,m \tag{3}$$

To avoid the difficulty in choosing appropriate learning functions, a learning function allocation strategy based on a reward mechanism is proposed. This approach continuously adjusts the selection of learning functions based on their historical performance and effectiveness in identifying informative samples to improve model accuracy. The reward function $r_l(k)$ for the lth learning function in the kth iteration is defined as:

$$r_l(k) = -\frac{\left|\hat{\mu}_{\hat{g}_E}(\hat{\boldsymbol{x}}_l)\right|}{f(\hat{\boldsymbol{x}}_l) * d^2(\hat{\boldsymbol{x}}_l)}, \quad \text{where} \quad \hat{\mu}_{\hat{g}_E}(\boldsymbol{x}) = \sum_{i=1}^{m} w_i \hat{\mu}_{\hat{g}_i}(\boldsymbol{x}) \tag{4}$$

where $\hat{\boldsymbol{x}}_l$ is the newly selected sample from the lth learning function, $f(\hat{\boldsymbol{x}}_l)$ is the probability density of $\hat{\boldsymbol{x}}_l$, $d(\hat{\boldsymbol{x}}_l)$ denotes the Euclidean distance to the existing samples in the design of experiments (DoE), and $\hat{\mu}_{\hat{g}_i}(\boldsymbol{x})$ represents the predicted mean of each surrogate $\hat{g}_i(\boldsymbol{x})$ in the ensemble model.

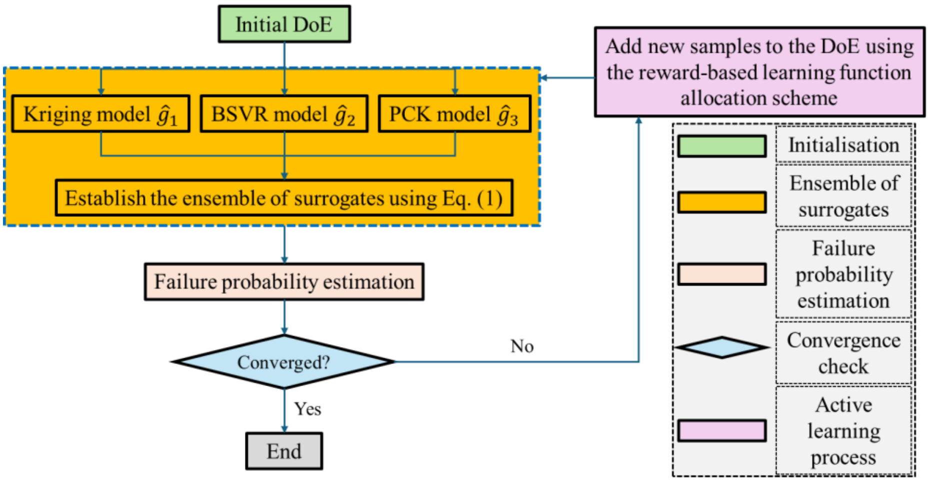

Figure 2. Overall workflow of proposed AEOS methodology.

This reward function is designed to prioritize sample selection near the limit state surface and in regions with high probability density while preventing excessive clustering with existing samples in the DoE, which is crucial for enhancing computational efficiency in active learning [16, 17]. In this study, six learning functions ($l = 6$) are used, and two samples are added in each iteration of AEOS to enable parallelization. With the availability of the surrogate model, failure probability is calculated using Monte Carlo Simulation (MCS) in each iteration.

The following stopping criterion for the active learning process is used:

$$\begin{cases} \Delta\hat{P}_f^i \leq \gamma_{P_f}, \quad \Delta\hat{P}_f^{i-1} \leq \gamma_{P_f}, \quad \Delta\hat{P}_f^{i-2} \leq \gamma_{P_f}, \quad i \geq 3 \\ \left|\frac{\hat{\beta}_i - \hat{\beta}_{i-1}}{\hat{\beta}_{i-1}}\right| < \epsilon_\beta \quad \text{and} \quad \left|\frac{\hat{\beta}_{i-1} - \hat{\beta}_{i-2}}{\hat{\beta}_{i-2}}\right| < \epsilon_\beta, \quad i \geq 3 \end{cases} \tag{5}$$

where $\Delta\hat{P}_f = \frac{\hat{P}_f^+ - \hat{P}_f^-}{\hat{P}_f}$ denotes the difference between the lower $\hat{P}_f^-$ and upper $\hat{P}_f^+$ bounds of failure probability, $\hat{\beta}_i$, $\hat{\beta}_{i-1}$, and $\hat{\beta}_{i-2}$ are the reliability indices (i.e. $\hat{\beta} = -\Phi^{-1}(\hat{P}_f)$, with $\Phi^{-1}(\cdot)$ denoting the inverse of standard normal CDF) estimated in the current, the $(i-1)$th, and the $(i-2)$th iterations, respectively. The threshold values γ_{P_f} and ϵ_β are taken as 0.1 and 1×10^{-3}, respectively. In the fatigue reliability analysis of OWTs, the performance function over T years of operation can be given as follows [4]:

$$g(V_w, H_s, T_p) = 1 - \frac{T * \mathcal{D}_c}{T_c} \tag{6}$$

where V_w, H_s, and T_p are mean wind velocity, significant wave height, and wave period, respectively. The distribution parameters of these variables are summarised in Table 1. Using the stress time series obtained from the FE model, fatigue damage is assessed through the rainflow counting method to identify stress cycles. The fatigue life is estimated based on *S-N* curves. Then, the cumulative damage $\mathcal{D}_c$ over a given time interval T_c is evaluated using the Palmgren-Miner rule. Following wind turbine design standards, a 600 s simulation is used in this study [4].

Table 1. Distribution parameters of random variables in the OWT.

Random variable	Distribution	Mean	Coefficient of variation
Mean wind velocity V_w	Weibull	4.85 m/s	0.6
Significant wave height H_s	Lognormal	0.35 m	0.82
Wave period T_p	Lognormal	4.9 s	0.33

4. OWT RELIABILITY PREDICTION

The fatigue reliability of the OWT was evaluated using five methods: importance sampling (IS), subset simulation (SS), second-order reliability method (SORM), adaptive kriging-based MCS (AK-MCS), and the proposed AEOS. For the case with $T = 20$ years, the results of the fatigue reliability analysis using different methods are listed in Table 2. The reference result is calculated from importance sampling and the failure probability is estimated as 0.1159 with a coefficient of variation of 2.5% using 2753 FE simulations, requiring over 40 hours of computational time.

Table 2. Fatigue reliability analysis results (T=20) of the OWT using different methods.

Methods	$\hat{P}_f$	$\hat{\beta}$	N_f	$\epsilon_{\hat{P}_f}(\%)$	Time
IS	0.1159	1.196	2753	–	40h44m20s
SS	0.1158	1.196	1813	0.09	27h27m2s
SORM	0.1070	1.242	76	7.68	1h3m39s
AK-MCS	0.1184	1.191	181	2.07	4h59m37s
AEOS	0.1161	1.195	42	0.17	38m58s

As shown in Table 2, SS provides a nearly identical estimate to IS, with a relative error of only 0.09%, but still requires a high number of FE simulations (1813) and a computational time exceeding 27 hours. Although SORM is computationally efficient, completing the analysis in approximately 1 hour, it underestimates the failure probability by 7.68%, demonstrating its limitations in capturing the nonlinear failure surface.

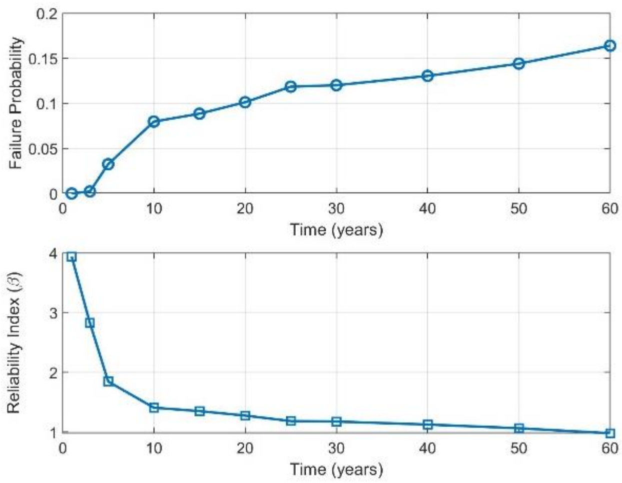

Figure 3. Variation of fatigue failure probability and reliability index of the OWT over time.

AK-MCS improves computational efficiency compared to IS and SS while maintaining an estimation with acceptable accuracy, reducing the required FE simulations to 181. However, it still requires nearly 5 hours to obtain the results, which may limit its practicality for large-scale applications. In contrast, the proposed AEOS method achieves a highly accurate failure probability estimate with a relative error of only 0.17% while significantly reducing computational cost. AEOS requires only 42 FE simulations and completes the analysis in approximately 39 minutes, demonstrating its superior efficiency and suitability for rapid fatigue reliability assessment.

The variation of failure probability and reliability index over the operational lifespan of the OWT is depicted in Fig. 3. The results indicate a progressive increase in failure probability, rising from 4.11×10^{-5} in year 1 to 0.1639 in year 60, while the reliability index declines correspondingly from 3.94 to 0.98. The most significant reduction in reliability occurs within the first 10 years, where the reliability index β declines from 3.94 to 1.41, reflecting the early-stage accumulation of fatigue damage under cyclic environmental loading. Beyond 20 years, the decline in reliability slows, with β decreasing marginally from 1.27 at year 20 to 1.06 at year 50, suggesting that the remaining structural capacity continues to degrade but at a reduced rate. The proposed AEOS framework provides an efficient tool for conducting rapid reliability assessments to support decision-making in OWT design and lifecycle management, facilitating the exploration of life extension strategies to ensure continued safe operation beyond the intended design life.

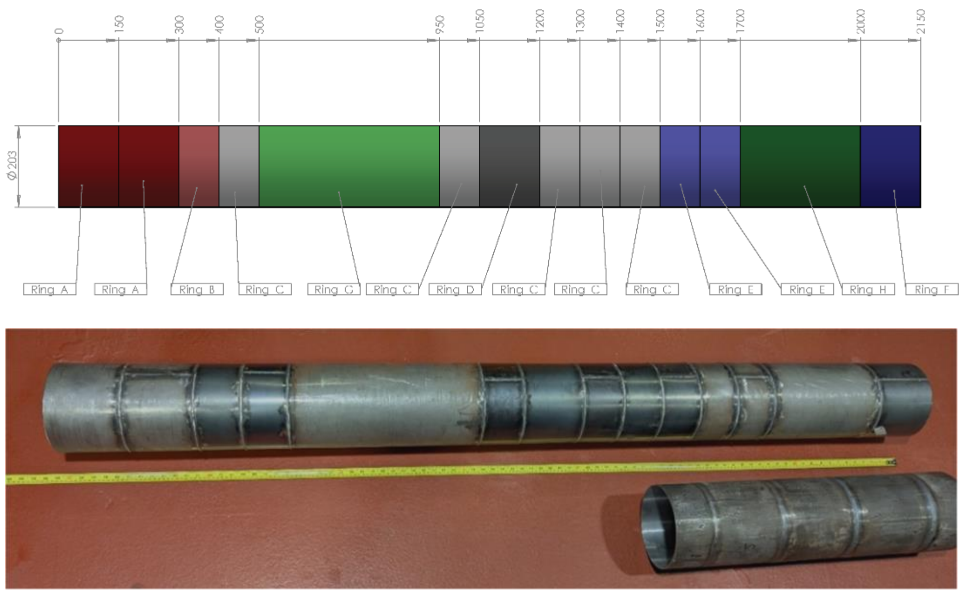

Figure 4. Schematic diagram and photograph of scaled monopile prototypes (dimensions in mm).

5. GUIDED WAVE MONITORING

Low frequency guided waves can propagate long distances [18], e.g., downwards along the monopile from permanently installed, piezoelectric sensors (between transition piece and splash zone), recording reflections at welds, corrosion, and developing fatigue cracks. Compared to traditional sensors, these can remotely monitor defects at critical locations below the mudline, thereby allowing a better characterization of the asset's remaining useful life (RUL) and updating of reliability analysis. However, the applicability of guided wave monitoring for large diameter monopiles with frequent circumferential welds as required by the manufacturing methodology has not been systemically investigated. Scaled prototypes for the laboratory testing were commissioned and manufactured, as shown in Fig. 4. Two different manufacturing techniques were employed to achieve the specific geometry and to ensure the prototype dimensions provided a sensible scaling of as-installed OWT monopiles. Preliminary measurements were conducted employing a laboratory setup [19] to quantify the guided wave propagation along the steel prototypes.

6. CONCLUSIONS

This study presents an adaptive ensemble of surrogate models (AEOS) for fatigue reliability analysis of offshore wind turbines (OWTs). The effectiveness of AEOS was demonstrated for the fatigue reliability assessment of a reference monopile-supported OWT. AEOS provided highly accurate failure probability estimates with significantly reduced computational costs, highlighting its potential for large-scale structural reliability evaluations. The results indicate a progressive decline in OWT reliability over time due to accumulated fatigue damage under cyclic environmental loading. This underscores the need for enhanced fatigue-resistant design, proactive maintenance strategies, and life extension measures to ensure continued safe operation. The feasibility of employing guided ultrasonic waves to monitor the inaccessible, submerged part of the monopiles to detect the development of critical defects was proposed. By integrating SHM data with probabilistic fatigue analysis, the proposed approach offers a powerful tool for risk-informed decision-making, supporting the sustainable management of offshore wind assets beyond their original design life.

REFERENCES

[1] Díaz, H. and Soares, C.G., "Review of the current status, technology and future trends of offshore wind farms," Ocean Engineering **209**, 107381 (2020). https://doi.org/10.1016/j.oceaneng.2020.107381

[2] Liao, D., Zhu, S.P., Correia, J.A., De Jesus, A.M., Veljkovic, M. and Berto, F., "Fatigue reliability of wind turbines: historical perspectives, recent developments and future prospects," Renewable Energy **200**, 724-742 (2022). https://doi.org/10.1016/j.renene.2022.09.093

[3] Nielsen, J.S. and Sørensen, J.D., "Risk-based derivation of target reliability levels for life extension of wind turbine structural components," Wind Energy **24**, 939-956 (2021). https://doi.org/10.1002/we.2610

[4] Yu, Q. and Xu, J., "Fatigue reliability assessment of Floating Offshore Wind Turbines under correlated wind-wave-current loads," Ocean Engineering **313**, 119442 (2024). https://doi.org/10.1016/j.oceaneng.2024.119442

[5] Wang, L., Kolios, A., Liu, X., Venetsanos, D. and Cai, R., "Reliability of offshore wind turbine support structures: A state-of-the-art review," Renewable and Sustainable Energy Reviews **161**, 112250 (2022). https://doi.org/10.1016/j.rser.2022.112250

[6] Seo, J., Pokhrel, J. and Hu, J.W., "Multi-hazard fragility analysis of offshore wind turbine portfolios using surrogate models," Renewable and Sustainable Energy Reviews **165**, 112552 (2022). https://doi.org/10.1016/j.rser.2022.112552

[7] Slot, R.M.M., Sørensen, J.D., Sudret, B., Svenningsen, L. and Thøgersen, M.L., "Surrogate model uncertainty in wind turbine reliability assessment," Renewable Energy **151**, 1150-1162 (2020). https://doi.org/10.1016/j.renene.2019.11.101

[8] Zhao, G., Dong, S. and Zhao, Y., "Fatigue reliability analysis of floating offshore wind turbines under the random environmental conditions based on surrogate model," Ocean Engineering **314**, 119686 (2024). https://doi.org/10.1016/j.oceaneng.2024.119686

[9] Wilkie, D. and Galasso, C., "Gaussian process regression for fatigue reliability analysis of offshore wind turbines," Structural Safety **88**, 102020 (2021). https://doi.org/10.1016/j.strusafe.2020.102020

[10] Huchet, Q., Mattrand, C., Beaurepaire, P., Relun, N. and Gayton, N., "AK-DA: An efficient method for the fatigue assessment of wind turbine structures," Wind Energy **22**, 638-652 (2019). https://doi.org/10.1002/we.2312

[11] Ren, C., Aoues, Y., Lemosse, D. and Souza De Cursi, E., "Ensemble of surrogates combining Kriging and Artificial Neural Networks for reliability analysis with local goodness measurement," Structural Safety **96**, 102186 (2022). https://doi.org/10.1016/j.strusafe.2022.102186

[12] Wang, J., Li, C., Xu, G., Li, Y. and Kareem, A., "Efficient structural reliability analysis based on adaptive Bayesian support vector regression," Computer Methods in Applied Mechanics and Engineering **387**, 114172 (2021). https://doi.org/10.1016/j.cma.2021.114172

[13] Schobi, R., Sudret, B. and Wiart, J., "Polynomial-chaos-based Kriging," International Journal for Uncertainty Quantification **5**, 171-193 (2015). https://doi.org/10.1615/Int.J.UncertaintyQuantification.2015012467

[14] Jonkman, J., Butterfield, S., Musial, W. and Scott, G., "Definition of a 5-MW reference wind turbine for offshore system development," NREL/TP-500-38060. National Renewable Energy Lab, Golden, CO (United States) (2009). https://doi.org/10.2172/947422

[15] Chen, C., Duffour, P., Fromme, P. and Hua, X., "Numerically efficient fatigue life prediction of offshore wind turbines using aerodynamic decoupling," Renewable Energy **178**, 1421-1434 (2021). https://doi.org/10.1016/j.renene.2021.06.115

[16] Wang, J., Xu, G., Yuan, P., Li, Y. and Kareem, A., "An efficient and versatile Kriging-based active learning method for structural reliability analysis," Reliability Engineering & System Safety **241**, 109670 (2024). https://doi.org/10.1016/j.ress.2023.109670

[17] Wang, J., Cao, Z., Xu, G., Yang, J. and Kareem, A., "An adaptive Kriging method based on K-means clustering and sampling in n-ball for structural reliability analysis," Engineering Computations **40**, 378-410 (2023). https://doi.org/10.1108/EC-12-2021-0705

[18] Loveday, P.W. and Fromme, P., "Low-cost instrumentation for high frequency ultrasonic guided wave laboratory research in free rock bolts," Applied Acoustics **227**, 110262 (2025). https://doi.org/10.1016/j.apacoust.2024.110262

[19] Li, L. and Fromme, P., "Mode conversion of fundamental guided ultrasonic wave modes at part-thickness crack-like defects," Ultrasonics **142**, 107399 (2024). https://doi.org/10.1016/j.ultras.2024.107399